The International Journal of Engineering and Science (IJES)
|| Volume || 12 || Issue || 3 || March || Pages || PP 46-54 || 2023 ||
ISSN (e): 2319-1813 ISSN (p): 20-24-1805

HEAT AND FLUID FLOW MODELLING OF HYBRID OVEN USING LOW-REYNOLDS NUMBER TURBULENCE MODEL

G.C Nzebuka[1] and C.P Egole[2]

1. Department of Mechatronics Engineering Federal University of Technology Owerri

Email address: gaius.nzebuka@futo.edu.ng

2. Department of Materials and Metallurgical Engineering Federal University of Technology Owerri

ABSTRACT

A hybrid oven for efficient heat transfer process during drying of food stuff like meat and fish is highly needed, especially one with a cost effective fuel will be an ideal product for local farmers and small scale food processes units. In order to understand how heat transfer and fluid flow will affect the drying processes a two dimensional steady state finite volume model is employed to simulate the buoyancy driven turbulent flow in a hybrid oven powered by charcoal. The result reveals that the oven should be used for drying and processing food materials that have processing temperature of lower or equal to 237°C, and the drying materials should be place at a distance lower or equal to 0.305m for maximum heat transfer to the stock materials. Further investigation reveals that one side of the oven section will receive higher heat transfer rate as a result of the placement of the charcoal combustion chamber. Thus it is deduced that increasing the size of the heating chamber increases overall temperature of the flue gases in the oven thereby resulting in efficient heat transfer rate

Date of Submission: 15-03-2023 Date of Acceptance: 30-03-2023

I. INTRODUCTION

HEAT transport has been established to be the key phenomenon in most of industrial processes involving thermal processing of materials and components of engineering importance. The extent and degree of heat transfer for such processes is determined by the thermal properties of the materials involved. Oven design and manufacturing is one of such processes that need to implement models of thermal energy transport for optimum performance and high efficiency. Such ovens, kilns or furnaces can be used for hardening, drying or baking of materials, hence, study of fluid and temperature distribution within the oven becomes inevitable. Successful analysis of oven performance must incorporate fundamental basic knowledge of heat and mass transfer phenomena.

Several studies involving experimental and numerical approaches have been undertaken to elucidate the physics and mechanisms of dissipation of thermal energy and how it affects various thermo-mechanical industrial processes. However, experimental study of such processes is highly limited in literature probably because of cumbersomeness of measurements and difficulty of precision and accuracy in analytical description of all the combined modes of heat transfer. Coupled with cost implication and high time required for experimental investigations, many researchers opt for mathematical simulation and modelling using computational fluid dynamics (CFD).

Banooni *et al*. (2008) experimentally determined the heat transfer and quality aspects for baking of flat bread in an impingement oven. They instrumented the test facility to monitor and record during the baking process. Image processing was used for monitoring the bread volume and surface colour changes during baking. A number works on numerical modelling and simulation of oven processes have been reported in literature. Charette *et al*. (1987) developed a model using a numerical-mathematical method for the purpose of analyzing the performance of the ring furnace and the effect of various operational parameters on energy consumption, furnace behaviour and product quality. The model combines an energy balance on the gaseous stream and a

calculation of heat transfer inside the solids. The process is a semi-continuous counterflow heat exchange, further complicated by other phenomena such as air infiltration into the flue, evolution of volatile matter, and heat losses and this would have been too complicated to consider experimentally. Maina *et al.* (2017) reported on modelling and simulation of a solar brick oven for baking of bread. They used computational fluid dynamics (CFD) software, GAMBIT and FLUENT to simulate solar brick oven with the ultimate goals of cost effectiveness and environmental friendliness of the solar energy. They applied the well-known K-e and turbulence models and other partial differential equations to describe the problem. Uros *et al.* (2017) developed a numerical method of the shortbread baking process in a forced convection oven. They considered convective and radiative heat transfer models, the numerical models were validated by performing experimental measurements of temperature and carried out baking tests of the shortbread. Nicolas *et al.* (2010) modelled heat and mass transfer in bread during baking using Comsol multiphysics. Their model predicts pressures, temperatures and water contents evolutions in the dough for different energy requests. Michele and Alessio (2017) carried out thermal and fluid dynamic analysis of an air-forced convection rotary bread-baking oven by means of an experimental and numerical approach. Jacek et al. (2013) experimentally validated a CFD model for a heating oven with natural air circulation. They used 3-D computational fluid dynamics model and presented an experimental analysis of the flow and thermal processes within a laboratory heating oven with a natural air circulation.

In this present work, modelling and simulation of heat and fluid flow for a hybrid charcoal and electric powered oven is presented. This is thought to be useful because we are in a continent and country where 35%-40% of its population still rely on firewood for domestic cooking. If well analysed, this oven can be extended to small and medium scale enterprises (SMEs) for cost effectiveness and sustainability of our microeconomic indicators. The focus of the study will be on modelling and simulation of heat and fluid flow in an oven that can be powered by charcoal using the v2-f low-Reynolds number turbulence model. Though the oven is constructed (see figure 1) in such a way that it has two heating chambers, one section is for charcoal heating compartment when there is failure in power supply by national electric authority and the other section is for

electrical heating by means of electrical induction coils. But this study focuses on the analysis of heat and fluid flow in the natural convection regime when charcoal heating is in operation and electrical compartment is off perhaps due to power outage. The v2-f low-Reynolds number turbulence model has not been used to analyse or study the heat and fluid transport in the oven or furnaces to the best knowledge of the current researchers. The oven designed for this study can be used for cooking, baking and other drying food purposes.

Figure 1: the finished constructed oven

2.0 Computational Domain

A two dimensional schematic diagram of a sectional view of the physical domain is shown in Figure 1. The computational domain is only occupied by flue gases which is we assumed to be a Boussinesq fluid (air) with a reference temperature that is specified to be outside temperature ((313K) in order to accurately account for buoyancy effects.

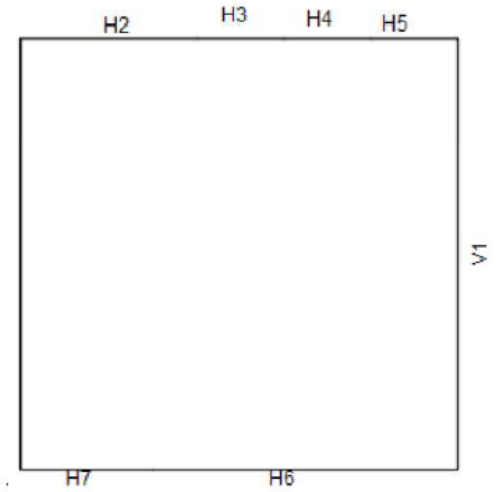

Figure 2: Two-Dimensional Computational Domain

Table1: Description of the Computational Domain with Dimensions and Boundary Conditions

SECTION SYMBOL	DIMENSIONS	SECTION NAME	BOUNDARY CONDITIONS
H2	1cm	Flue gas outlet	P_{Gauge}=0, T_{Exit}=505K (measured in 6180secs)
H3	1cm	Flue gas outlet	P_{Gauge}=0, T_{Exit}=505K(measured in 6180secs)
H4	1cm	Flue gas outlet	P_{Gauge}=0, T_{Exit}=505K(measured in 6180secs)
H5	12.345cm	Top Wall	Convective Boundary
H6	40.01cm	Electrical heating section wall	Convective Boundary
H7	11.014cm	Charcoal heating section inlet	P_{Gauge}=P_{atm}, Mass flow rate, T=T_{gas}
V1	61.127cm	Furnace Vertical wall	Convective Boundary

2.1 BOUNDARY CONDITIONS

The boundary conditions is as specified in the table 1, the inlet mass flow rate will be calculated, and the convective heat transfer coefficient at the convection boundaries was determined by means of empirical relations for both vertical and horizontal enclosures as shown elsewhere (Cengel 1998). The free stream temperature that will be incorporated in the convection boundaries is the ambient temperature (313K). The V1 label is also the same boundary condition at the left vertical wall (the unlabelled wall), as shown in the domain of figure 2. The electrical heating section was set to convection wall boundary being that the electrical chamber is in off mode during this analysis. Any other unlabelled section in the computational domain (figure 2) are taken to be convection wall boundaries for the oven

2.2 Numerical Model

From Reynolds-Averaged Navier-Stokes (RANS) equation for indoor air flow, the turbulent fluctuations are taking at averaged properties of the mean flow [19]. Following this approach, all the unsteadiness is averaged out by taking them as a part of the turbulence [20]. The time average flue gas velocity, pressure and temperature distribution in the attic space in our physical model as given in figure 2 are governed by the following steady-state continuity, momentum, and energy equations:
Continuity;

$$\frac{\partial}{\partial x_j}(\rho \bar{u}_i) = 0 \quad (1)$$

Momentum;

$$\frac{\partial}{\partial x_j}(\rho \bar{u}_i \bar{u}_j) = -\frac{\partial P}{\partial x_i} + \frac{\partial}{\partial x_j}\left[(\mu + \mu_t)\frac{\partial \bar{u}}{\partial x_j}\right] + \left(-\frac{\partial \overline{u'_i u'_j}}{\partial x_j}\right) - \rho g_i(T - T_\infty) \quad (2)$$

Energy;

$$\frac{\partial}{\partial x_j}(\rho c_p T u_i) = \frac{\partial}{\partial x_j}\left[\left(k_t + \frac{c_p \mu_t}{\sigma_T}\right)\frac{\partial T}{\partial x_j}\right] + \left(-\frac{\partial \overline{u'_i T'}}{\partial x_j}\right) \quad (3)$$

2.2.1 Turbulence Model

The study of natural convection has been investigated using low Reynolds turbulence k-ε turbulence model. The low Reynolds turbulence k-ε turbulence model might give rise to treatment of wall effect; therefore, suitable modifications like adding damping function and source terms in the regions within the vicinity of solid wall where there is a transition from laminar to turbulent region. A model originally proposed by Durbin 1991 called v2−f (v2f) model is used in this study. The v2f model is capable of handling the wall region without the need for the additional damping functions, since normal velocity fluctuations are known to be quite sensitive to the presence of wall and thus are like a natural damper (Durbin 1991).The model therefore does not require a low Re version to treat the presence of wall. The turbulence kinetic energy, k, its dissipation rate, ε, the velocity variance scale, $\overline{v^2}$ and the elliptic relaxation function, f, are obtain from the following four transport equations to ensure closure of RANS turbulence model equations:

Turbulence Kinetic Energy;

$$\frac{\partial}{\partial x_j}(\rho k \bar{u}_j) = P - \rho\varepsilon + \frac{\partial}{\partial x_j}\left[\left(\mu + \frac{\mu_t}{\sigma_k}\right)\frac{\partial k}{\partial x_j}\right] \quad (4)$$

Dissipation Rate;

$$\frac{\partial}{\partial x_j}(\rho \varepsilon \bar{u}_j) = \frac{C'_{\varepsilon 1} P - C_{\varepsilon 2}\rho\varepsilon}{T} + \frac{\partial}{\partial x_j}\left[\left(\mu + \frac{\mu_t}{\sigma_\varepsilon}\right)\frac{\partial \varepsilon}{\partial x_j}\right] \quad (5)$$

Velocity Variance Scale;

$$\frac{\partial}{\partial x_j}(\rho \overline{v^2}\, \bar{u}_j) = \rho k f - 6\rho \overline{v^2}\,\frac{\varepsilon}{k} + \frac{\partial}{\partial x_j}\left[\left(\mu + \frac{\mu_t}{\sigma_k}\right)\frac{\partial v^2}{\partial x_j}\right] \quad (6)$$

Elliptic Relaxation Function;

$$f - L^2\frac{\partial^2 f}{\partial x_j^2} = C_1 - 1\frac{\frac{2}{3} - \frac{\overline{v^2}}{k}}{T} + C_2\frac{P}{\rho k} + \frac{5\overline{v^2}/k}{T} \quad (7)$$

Where,

$$P = 2\mu_t S^2, \qquad S^2 = S_{ij}S_{ij}, \qquad S_{ij} = \frac{1}{2}\left(\frac{\partial u_i}{\partial x_j} + \frac{\partial u_j}{\partial x_i}\right) \quad (8)$$

The turbulence time scale T and length scale L are defined by

$$T' = \max\left[\frac{k}{\varepsilon}, 6\sqrt{\frac{\nu}{\varepsilon}}\right] \quad (10)$$

$$T = \min\left[T', \frac{\propto}{\sqrt{3}\,\overline{v^2}C_\mu\sqrt{2S^2}}\right] \quad (11)$$

$$L' = \min\left[\frac{k^{\frac{3}{2}}}{\varepsilon}, \frac{1}{\sqrt{3}}\frac{k^{\frac{3}{2}}}{\overline{v^2}C_\mu\sqrt{2S^2}}\right] \quad (12)$$

$$L = C_L \max\left[L', \quad C_\eta\left(\frac{v^3}{\varepsilon}\right)^{1/4}\right] \quad (13)$$

In the above equations, ∞,C_1,C_2, $C_{\varepsilon 1}$, $C'_{\varepsilon 1}$, $C_{\varepsilon 2}$, C_η, C_μ, and C_L are constants. σ_k, σ_ε and σ_T are the turbulent prandtl numbers for k, ε and T respectively. v is the kinematic viscosity (μ/ρ). The turbulence (or eddy) viscosity μ_t is defined as follows:

$$\mu_t = \rho C_\mu \overline{v^2} T \qquad (14)$$

2.2.2 Model Constants

The solid wall no-slip boundary conditions are: u= 0., k=∂nk =0, $\overline{v^2} = 0$.

Other model constants are as follows; ∞=0.6, $C_1 = 1.4$, $C_2 = 0.3$, $C_{\varepsilon 1} = 1.4$, $C_{\varepsilon 2} = 1.9$, $C_\eta = 70$, $C_\mu = 0.22$, $C_L = 0.23$, $\sigma_k = 1$, $\sigma_\varepsilon = 1.3$, $\sigma_T = 0.85$ $C'_{\varepsilon 1} = C_{\varepsilon 1}\left(1 + 0.045\sqrt{k}/\overline{v^2}\right)$ (15)

2.2.3 Measured and Calculated Physical Quantities

Baldwin (1987) determines charcoal chemical composition by mass experimentally to be;

Table 2: Composition of Charcoal By Mass Percentage

ELEMENT	C	H	O	N	Ash	S
% BY MASS	82	3.1	11.3	0.2	3.4	0

The theoretical air quantity is calculated based on the chemical reaction between the elements and oxygen. Assuming nitrogen is inert and does not participate in the combustion, likewise Ash.

Carbon combines with oxygen to form CO2 and heat

1. C + O2 → CO2 (i)
   $1C + \frac{32}{12}O \rightarrow \frac{44}{12}CO_2$ (ii)
   1kg + 2.67 kg Oxygen → 3.67 kg carbon dioxide
2. Hydrogen combines with oxygen to form water and heat
   $2H_2 + O_2 \rightarrow 2H_2O$ (i)
   $1H + \frac{32}{4}O \rightarrow \frac{36}{4}H_2O$ (ii)
   1Kg Hydrogen + 8KgOxygen → 9Kg Water
3. Theoretical Oxygen required to burn the charcoal is;
   2.67 X C% + 8 X H% - O%
   Percentage of C, H and O is given in table 2. Therefore,
   2.67 X 0.82 + 8 X 0.031 – 0.113
   This gives, 2.324 Kg of oxygen for 1kg of coal.

4. Theoretical Air required to burn the charcoal is;
   2.324 Kg/23.2% = 10.02Kg of Air for 1Kg of charcoal. 23.2% was used because air contains 23.2% by weight of oxygen.

Table 3: Measured Data for the Computation of the Furnace

Measured Physical Quantities	Values	Data Acquisition Method
Weight of the charcoal in the combustion chamber(Kg)	1.6	Weighing balance
Total fuel consumption time (hr)	3.5hr	Physical reading and timing
Average fuel consumption (Kg/hr)	0.457	Calculated
Theoretical air required to burn 1Kg of charcoal(Kg)	10.02	Calculated
Exit Flue gas temperature (K), T_{Exit}	505k	K-Type Thermocouple (measured in 6180secs)
Density of charcoal (Kg/m^3)	240	Available in online engineering toolbox
Ambient Temperature (K)	313	K-Type Thermocouple(measured in 6180secs)

Mass flow rate that was used in the inlet boundary condition;
Since 10.02Kg of air burns 1Kg of charcoal; 1.6Kg of charcoal will be burn by 16.032Kg of air, therefore, in every 3.5hours or 12600seconds; 16.032Kg/12600secs= 0.001272Kg/s of air will burn the charcoal. Which implies that the Mass Flow rate at the inlet boundary condition will be specified to be 0.001272Kg/s.

2.2.4 Solution Method

The governing equations and models formulated above was implemented by means of the commercial software ANSYS FLUENT. The scheme employed is coupled system for solving the pressure and velocity coupling so that pseudo transient scheme can be activated for solving the buoyance driven flow, and body force weighted is employed for spatial discretization of pressure, while second order upwind differencing was used for spatial discretization of velocities and scalar transport equations. Non-uniform quadrilateral dominant grids was employed, and the boundaries are inflated with nodes tightly clustered near the walls to ensure that the y+ value for the first grid closed to the wall is everywhere less than 0.8. A grid dependence test was conducted by comparing the result of a 26460 nodes and a 37520 nodes. It was discovered that the difference between the two grids in the wall heat transfer rate and total mass flow rate is less than 1%. So, in this study a modelling of a grids size of 26460 nodes were chosen.

3.0 Results and Discussion

Figure 3 is a Predicted numerical results for isotherms and streamlines. The predicted temperature distribution (figure 3a) is considered to be a combination of thermal boundary layers developed along the walls of the oven boundaries and thermal stratification occupying half of the oven space. The isotherms with higher values move toward the cold top walls and the outlet. The turbulent air flow in the oven is dominated by two by two convection cells (figure 3b). Air flow in the top left section is counter-clockwise and associated with stronger vortex as can be seen in the greater number of streamlines in that left top section. The flue gases nearer to the combustion chamber has lower density and needs to move upwards while on the other hand the fluid near to the non-combustion chamber needs to move downwards due to higher density. This causes the cavity to be divided into two with each unequal cells flowing and rotating in opposite direction. The air flow in the bigger cell at the right section of the oven is clockwise.

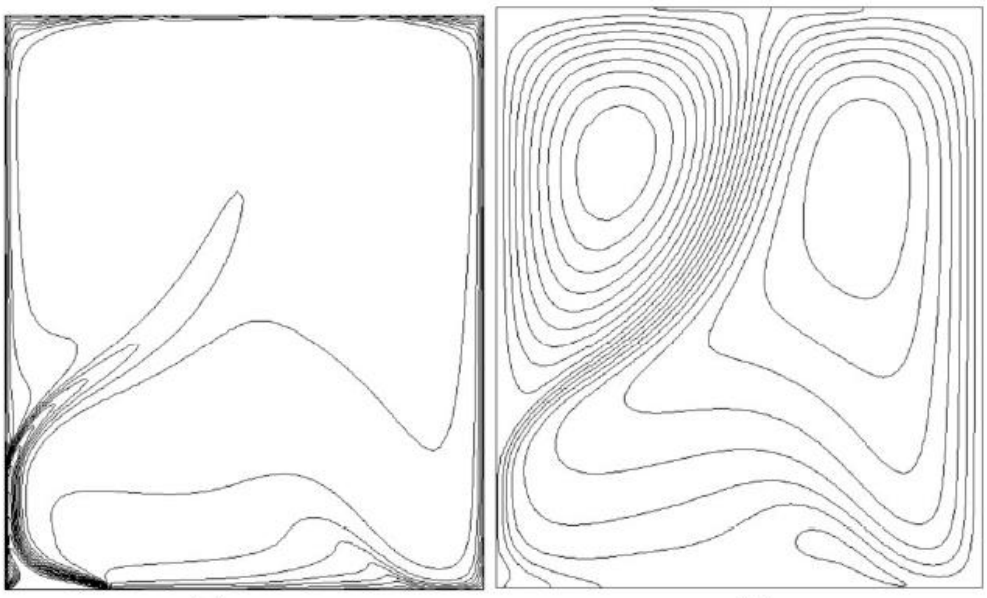

(a) (b)

Figure 3: Predicted (a) Isothermal Contour and (b) Streamline

The temperature peak figure 4 at a distance of about x=0.18m and y= 0.305m at the mid-section of the oven is 510K where flue gas velocity (0.505m/s) is both highest as seen in figure 5 and flow is upward. Both maximum temperature and maximum velocity regions are very close to the combustion sections of the oven. The velocity and temperature both decreases rapidly after the peak values, as the flow moves toward the cooler non-combustion section of the oven. The temperature everywhere within the space under the steady state condition assumed in this work is below 510K or237°C, which implies that any drying processes of more than 2hours which can be safely considered to be a longer time duration (for steady state consideration of this study to be valid) should not be processed with this charcoal heated oven capacity. Moreover, locating the rail for placing the drying stuffs at a distance below 0.305m should be recommended for maximum heat transfer from the flue gas by convection and walls by conduction and radiation to the drying materials.

The higher temperature seen in figure 6, plotted for the left vertical wall section of the oven corresponds to a minimum heat flux, this is because the temperature differences across the wall thickness reaches minimum there. However, the lower temperature seen in figure 7 along the vertical right side wall section of the oven indicates a maximum heat flux as the temperature difference across the wall thickness assumes a maximum value.

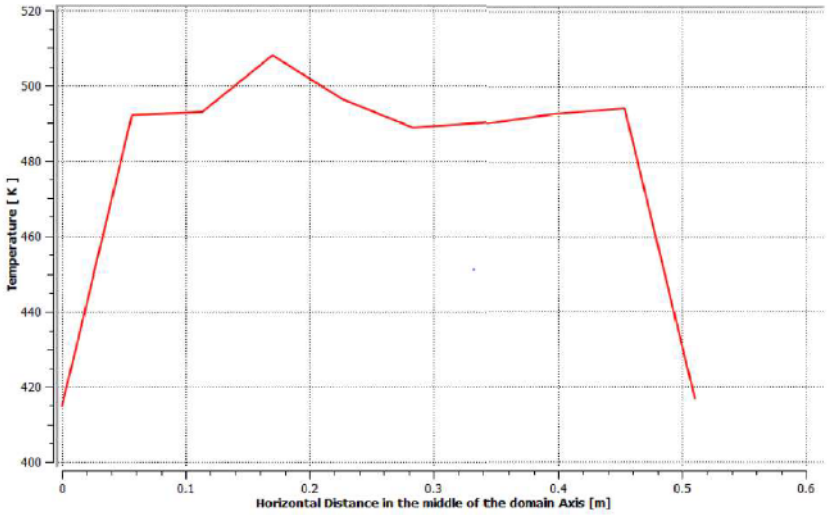

Figure 4: Predicted temperature profile along the middle horizontal section of the oven

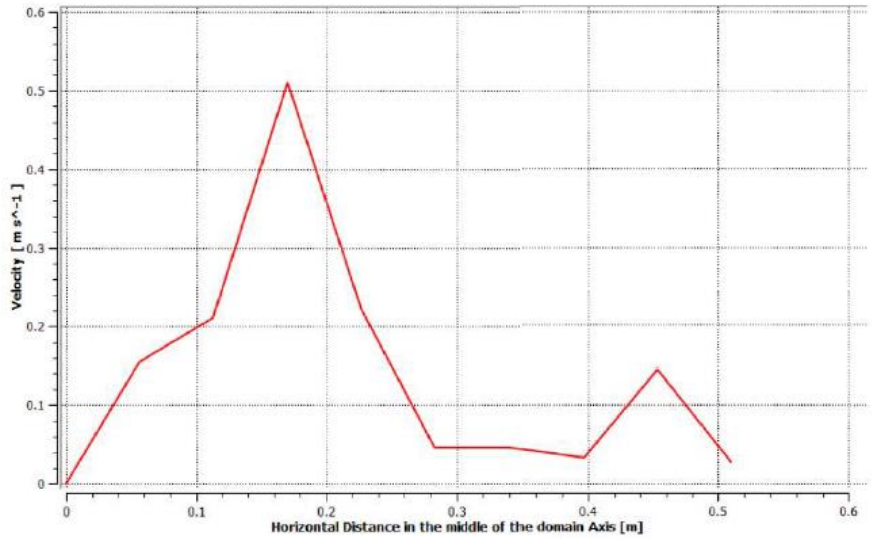

Figure 5: Predicted velocity profile along the middle horizontal section of the oven

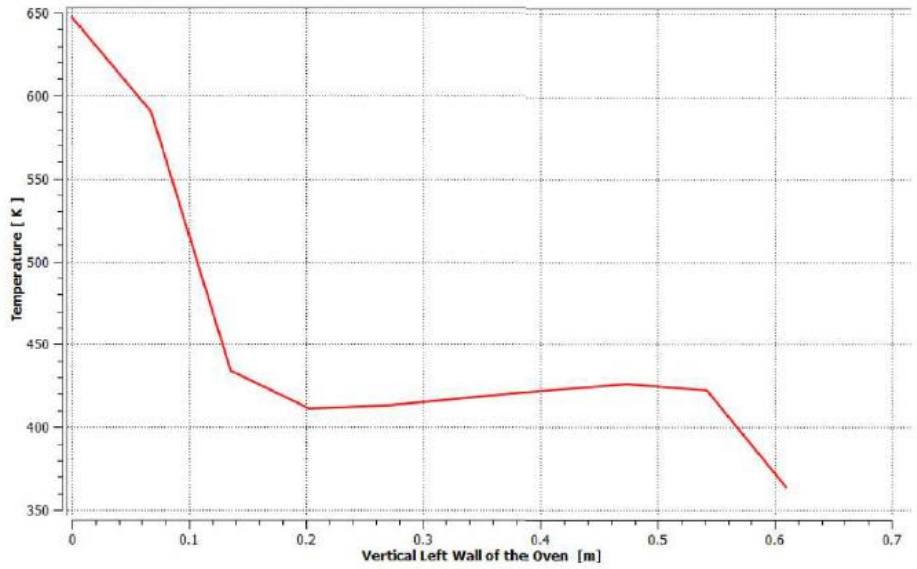

Figure 6: Predicted temperature profile along the middle vertical left section of the oven

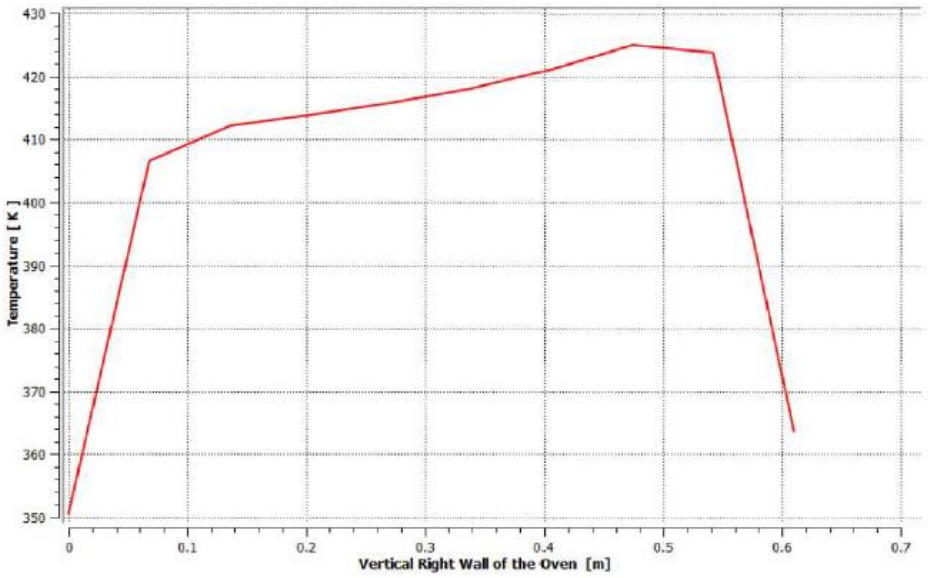

Figure 7: Predicted temperature profile along the middle vertical right section of the oven

4.0 CONCLUSION

Buoyancy-driven 2-D turbulent flow in the space of a hybrid oven heated by charcoal is simulated using a CFD model. The investigation reveals that the oven should be used for drying and processing food materials that have processing temperature of lower or equal to 237°C, and the drying materials should be place at a distance lower or equal to 0.305m for maximum heat transfer to the stock materials. Further investigation reveals that one side of the oven section will receive higher heat transfer rate as a result of the placement of the charcoal combustion chamber. Thus it is deduced that increasing the size of the heating chamber increases overall temperature of the flue gases in the oven thereby resulting in efficient heat transfer rate. For maximum exposure of the food stock for drying purposes, the stock should be stacked toward the left section (heating section) where it can have maximum contacts with the both heat of the flue gases and nearby wall.

References

[1] Banooni S., Hosseinalipour S.M., Mujumdar A.S., Taheran E., Bahiraei M., and Tarhekhani P., Baking of Flat Bread in an Impingement Oven: An Experimental Study of Heat Transfer and Quality Aspects, Taylor and Francis, Vol. 26, p.902-909, 2008.

[2] Baldwin, S.F. Biomass Stoves: Engineering Design, Development, and Dissemination. Volunteers in Technical Assistance, 1987.

[3] Bui R.T., Charette A., Bourgeois T., Dernedde E., Performance Analysis of the Ring Furnace used for Baking Industrial Carbon Electrodes, The Canadian Journal of Chemical Engineering, Vol.65, Issue 1, p.96-101 , 1987.

[4] Cengel, Y.A. Heat Transfer A Practical Approach, McGraw- Hill Higher Education p.411-433, 1998.

[4] Durbin, P. A. Near wall turbulence closure modelling without damping functions. Theory of Computational Fluid Dynamics 3(1), (1991) 1–13

[5] Jacet S., Zbigniew B., and Andrzej J.N., The Experimental Validation of a CFD Model for a Heating Oven with Natural Air Circulation, Applied Thermal Engineering, Elsevier, Vol. 54, p.387-398 , 2013.

[6] Maina M.B., Ngala G.M., and Abdulrahim A.T., Modelling and Simulation of Solar Brick Oven for Bread Baking, University of Maiduguri Faculty of Engineering Seminar Series Vol. 8, p.65-71 , 2017.

[7] Michele P. and Alessio S., Thermal and fluid dynamic analysis of an air-forced convection rotary bread-baking oven by means of an experimental and numerical approach, Applied Thermal Engineering, Elsevier, Vol. 117, p.330-342 , 2017.

[8] Nicolas V., Salagnac P., Glouannec P., Jury V., Boillereaux L., and Ploteau J.P., Modelling Heat and Mass Transfer in Bread during Baking, Proceedings of COMSOL conference 2010, Paris.

[9] Uros K., Leopold S., and Jure R., A Numerical model of the shortbread baking process in a forced convection oven, Applied Thermal Engineering, Elsevier, Vol. 111, p.1304-1311, 2017.